Anal. Bioanal. Electrochem., Vol. 15, No. 10, 2023, 874-890
https://www.doi.org/10.22034/abec.2023.708676

Analytical &
Bioanalytical
Electrochemistry

2023 by CEE
www.abechem.com

Full Paper

Electro-catalytic Activity Based MWCNT-tetraamino Zinc(II)phthalocyanine onto the Glassy Carbon Electrode Towards Determination of Bio-analytes: A Cyclic Voltammetric Study

Malathesh Pari*

Department of P.G, Studies and Research in Chemistry, Sahyadri Science College, Kuvempu University, Shimoga, 577203, Karnataka, India

*Corresponding Author, Tel.: +918147987899
E-Mail: malathshpari@gmail.com

Received: 22 April 2023 / Received in revised form: 7 October 2023 /
Accepted: 10 October 2023 / Published online: 31 October 2023

Abstract- This paper covers the synthesis and characterization of tetraamino Zinc(II) metallophthalocyanine (Zn(II)TAPc) using spectroscopic and electrochemical techniques. The electrochemical determination of dopamine (DA), ascorbic acid (AA) and uric acid (UA) was investigated using composite modified MWCNT-Zn(II)TAPc/GCE, due to their excellent conductivity, electrons transfer ability compared to the bare glassy carbon electrode (GCE), and because the charge transfer rate increases with multiwalled carbon nano tubes (MWCNT) on the surface of GCE. As a result, electrochemical sensing of bioanalytes was investigated on MWCNT-Zn(II)TAPc/GCE, and the analytical profile of micro molar concentration (µM) of DA is in the linear range of 0.1 to 1.1 µML^{-1} with LOD is 0.033µML^{-1}, sensitivity of 14.063 µAµML^{-1} and the electro analytical sensing of AA and UA while using modified composite electrode for AA the linear range of 0.2-0.7 µmol L^{-1}, LOD of 0.066µmol L^{-1} and sensitivity 54.821 µAµM^{-1} cm^{-2}, for UA the linear range of 0.05–1.2 µmolL^{-1}, lower detection limit of 0.066 µmolL^{-1} and sensitivity of 0.515 µAµM^{-1} cm^{-2}, The MWCNT-Zn(II)TAPc/GCE shows good repeatability, stability and reproducibility.

Keywords- Zinc(II)Tetra-amino phthalocyanine; MWCNTs; Dopamine; Ascorbic acid; Uric acid; Cyclic voltammetry

---

1. INTRODUCTION

It is believed that the Zn(II)TAPc is an 18π-electron conjugated aromatic metal phthalocyanine (MPc) compound that enhances quantification and has drawn researchers in a variety of domains including photodynamic therapy, solar cells, optical storage devices, semiconductors, and electrochemical detection, electrocatalytic activity and redox processes [1-4]. Zn(II)TAPc is known for its rich redox chemistry since it contains NH_2 and a central metal atom. Further, by tailoring MPc with the choice of a peripheral ligand with composite multiwalled carbon nanotubes (MWCNTs) material can provide target applications. Thus, MWCNTs-Zn(II)TAPc/GC composite electrodes are well known to show good electro-catalytic activity towards various electrochemical reactions [5–7]. The combination of MWCNT embedded with Zn(II)TAPc has recently been proposed as an excellent sensor platform due to its high electrical conductivity, very good mechanical strength, and large surface area, pore structure and chemical stability of carbon nanotube (CNT) in nanosheets [8-12].

Ascorbic acid (AA), Dopamine (DA) and Uric acid (UA) are bioanalytes that play important roles in human metabolism, as well as the neurological and renal systems. Since these three bioanalytes usually coexist in real biological matrices, AA is a vital component in human diet with the highest concentrations in animal organs such as liver, leukocytes, and anterior pituitary and it is present in the mammalian brain along with amine neurotransmitters and DA. In addition, AA is a water-soluble Vitamin-C and a compound involved in several vital body functions. This vitamin is often added to different foods and medicines owing to its antioxidant properties and pH-regulating abilities [13].

Besides, DA is an important catecholamine neurotransmitter molecule in the brain and its deficiency causes brain disorders such as Parkinson’s and schizophrenia and recently, the identification and determination of AA and DA by electrochemical methods has attracted much attention as well [14-16]. However, it is difficult to determine AA by direct oxidation on bare GCE because of the high potential and the fouling effects of its oxidation products [17]. Also, the AA and DA waveforms have nearly the same potential and overlap, resulting in poor selectivity and reproducibility. Furthermore, UA is a byproduct of purine metabolism. Many diseases are caused by its abnormal concentration in the body such as gout, hyperuricaemia and Lesch-Nyan disease. Elevated levels of UA in serum cause kidney damage and cardiovascular disease. Therefore, the study of determining the UA is in fact very essential and also both UA and AA are present in biological fluids such as blood and urine [18].

On the other hand, electrochemical methods provide more promising results than fluorometric, chromatographic, spectrophotometric or capillary electrophoresis methods [19-21]. Earlier electrochemical procedures based on the oxidation of UA at carbon-based electrodes in acidic solutions suffered from interference from AA which can be oxidized at a potential close to that of UA. Varied methods, such as an adsorption/medium exchange approach, enzyme-based techniques, chemically modified electrodes were developed to solve the UA sensing problem [22-26]. In spite of the importance of UA in pharmaceuticals, sensitive and selective methods remain to be developed as each of these proposed methods has its own set of advantages and disadvantages.

The development of chemically drop-coated electrodes represents a growing area of research in analytical chemistry and electrochemistry, with diverse applications. Some modified electrodes have been used to investigate electrochemical behavior of biomolecules. Ling Mei Niu et al [27] have studied electrochemical behavior of UA at Meso-2, 3-Dimercaptosuccinic acid self-assembled gold electrode [7]. Zonghua Wang group have modified graphite electrode for the simultaneous determination of DA and AA [8]. Alanine covalently modified glassy carbon electrode was used to study AA and DA [5]. Simultaneous Electroanalysis of DA, AA and UA by poly (vinyl alcohol) covalently modified glassy carbon electrode has also been accomplished [25] along with simultaneous determination of DA and serotonin in presence of AA and UA at poly (*O*-phenyl diamine) modified electrode [26].

Using electro-organic reactions as a research tool, we are expanding our work on biosensors [28-32]. Hence in this work, we report the drop coated GCE with Zn(II)TAPc, MWCNTs-Zn(II)TAPc/GCE and the structure of composite materials were evaluated by IR, UV-Vis, XRD, TGA, SEM analysis and further the modified electrodes successfully determine the bioanalytes like DA, AA and UA individually via CV technique exhibiting well-defined characteristics peaks and the selectivity of the proposed method is better than the previous ones is strongly justified our existing work.

2. EXPERIMENTAL SECTION

2.1. Chemicals

All chemical compounds were of the analytical grade and were utilized directly throughout without the analysis, water that has been doubly distilled water was used throughout the experiments. Phosphate buffer solutions (PBS) were made in lab using reported procedure. DMF, $C_8H_{11}NO_2$ (DA), HC_6H7O_6 (AA), $C_5H_4N_4O_3$ (UA), DMSO, CH_4N_2O urea, NH_4Cl, ammonium molybdate ($(NH_4)_6Mo_7O_{24}$), the above-mentioned chemicals were purchased from Sigma (Sigma Aldrich GmbH, Sternheim, Germany). All reactions were conducted in dry N_2 environment.

2.2. Instruments

Using the (CV) electrochemical analyzer CHI620E model, electrochemical analysis was carried out using a three-electrode conventional system made up of a working electrode GCE, a platinum electrode serving as a counter electrode, and a saturation calomel electrode serving as a reference electrode. Nitrogen (N_2) was passed into the buffer solution to be deaerated, and oxygen molecules were redissolved. The thermal stability of the synthesized MPc was measured by TGA using a STA6000 device in the temperature range of 30–800 ^{0}C with a scan rate of 10°C min^{-1} under oxygen flow (30 mL min^{-1}). UV spectra were recorded on a SYSTRONICS UV-VIS Spectrophotometer 119. FT-IR spectra were recorded on a Perkin-Elmer Spectrum One FT-IR spectrometer with ATR capability, Powder X-Ray Diffraction spectra were recorded on Rigaku Japan Smart Lab 9 KW.

2.3. Synthesis of Zinc(II)tetra amino phthalocyanine Zn(II)TAPc

In order to preparation of Zn(II)TAPc, the basic compound zinc(II)tetra-nitro phthalocyanine is reduced with sodium sulfide(Na_2S) as previously discussed [33,34]. After the solid crude product of Zn(II)TAPc was removed and purified with ethanol, Eventually, the product was then washed with hot water and then with an alkali solution, the dark green products were dried over P_2O_5, the structure of MPc as shown in Figure 1 and subjected for physicochemical evaluation. Anal. Calcd. for $C_{56}H_{46}N_{12}O_4Zn$: C, 66.53; H, 4.55; N, 16.63; Zn, 5.84 %. Found: C, 66.97; H, 4.82; N, 16.39; Zn, 5.81.

2.4. Preparation of Zn(II)TAPc–MWCNTs hybrid materials

The composite materials Zn(II)TAPc–MWCNTs were synthesized using single step method (Figure 1). The following methods were used to prepare hybrid chemical composite material: MWCNTs were sonicated in nitrating mixture (3:1 by volume) for 8 hours at 80^{0}C. The obtained MWCNTs (0.05 g) were then refluxed in excess $SOCl_2$ (50 mL) for 24h at 70^{0}C. Distillation was used to remove the excess $SOCl_2$, and the residual solid was dried in the vacuum. The resulting solid was treated with Zn(II)TAPc (0.2 g) in 10 mL DMF. The excess Zn(II)TAPc was entirely removed by washing with hot water followed by acetone. The final composite hybrid materials were obtained by drying this solid at appropriate temperature.

2.5. Fabrication of biosensor

The glassy carbon electrode was cleaned first using Al_2O_3 suspension on a polishing pad with deaerated H_2O, followed by dilute acids, alkali solution, ethanol and then purified distilled water and dried at room temperature. For the modification of GCE, 0.5 ml IPA, 10 µL 2 wt% Nafion solution 0.5 mg Zn(II)TAPc were added. The mixture was then sonicated for 30 min to obtain a dispersed homogeneous suspension. 05 µL of a dispersed suspension were drop cast onto the clean GCE surface and let to air dry. As before, the Zn(II)TAPc–MWCNTs (composite sensor) was made by combining 1.0 mg of MWCNT and 05 mg of Zn(II)TAPc in 0.5ml IPA. To prevent oxygen interference, N_2 atmosphere was used for all electrochemical experiments

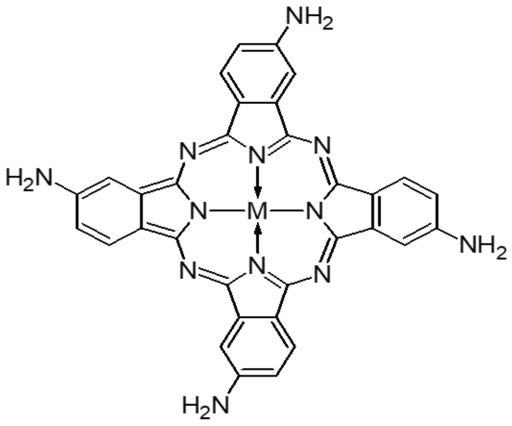

Figure 1. Structure of Tetra Amino Zn(II)Phthalocyanine **(**Zn(II)TAPc)

3. RESULTS AND DISCUSSION

3.1. Electronic spectra

Figure 2 shows the absorption spectra of the compounds MWCNT (block color), MWCNTs-Zn(II)TAPc (red color), and Zn(II)TAPc (blue color) in DMF. The electronic spectrum of visible light at 260-800 nm, the 630–740 nm monomeric Q-band of MWCNTs, MWCNTs-Zn(II)TAPc, Zn(II)TAPc is seen from Figure 2. The curves MWCNT (block colure), MWCNTs-Zn(II)TAPc (red color), and Zn(II)TAPc (blue color) is caused by the π-π^* transition and UV region at approximately 300–400 nm (Soret-band). While the additionally confirmed a few shoulders peak of both composite and non-composite materials. A broadened or split Q-band, with the high to the energy band in the range of 640 nm to 600 nm region. Aggregation in Zn(II)TAP is typified by being caused by the aggregate and the low energy band due to the monomer. In the MWCNTs-Zn(II)TAPc spectrum, the Q-band appears as one very broad aggregated form peak at 650nm; this also provides evidence for the monomeric properties of MWCNTs-Zn(II)TAPc. The spectroscopic data confirmed by the coupling of the three species (Zn(II)TAPc, MWCNT and MWCNTs-Zn(II)TAPc) [35,36].

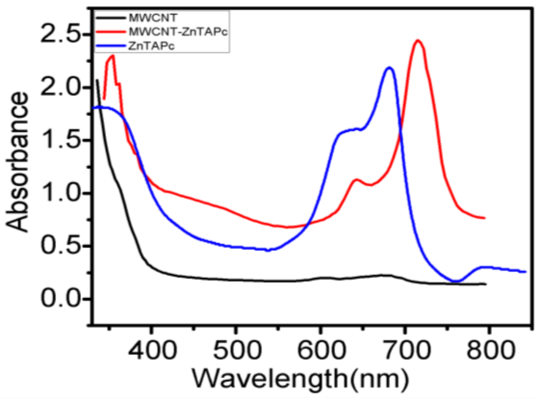

Figure 2. Absorption spectra of the compounds MWCNT, MWCNT-Zn(II)TAPc, Zn(II)TAPc

3.2. IR spectra

Using the fundamental KBr palates method, the IR spectrum was used to determine the chemical composition of MWCNT, Zn(II)TAPc and MWCNT-Zn(II)TAPc. Amide and the amide linkages between Zn(II)TAPc and MWCNTs were attributed to the peaks at 1738 and 1630 cm^{-1}, respectively. The sharp peak that appeared at 3450 cm$^{−1}$ was assigned to the –NH_2 moiety in Zn(II)TAPc and the disappearance of the -NH_2 peak and the appearance of a new peak at 3322 cm$^{−1}$ shows the formation of the proposed MWCNT-Zn(II)TAPc is shown in Figure 3. The stretching vibrations of (C=N) and (C=C) group were observed near 1726-1615 and 1496-1467 (C=O, C=N), 1388 (C-C), 1283, 1226, 1154, 1118, 1071, 932, 848, 638, 578, 543 and 459 cm$^{−1}$ inset Figure.3. The stretching vibrations of the un-composite and composite materials produce different vibrations. IR spectrum measurements support the hypothesized target structure, and These peaks are attributed to the various skeletal vibrations of MWCNT-Zn(II)TAPc and Zn(II)TAPc [37-39].

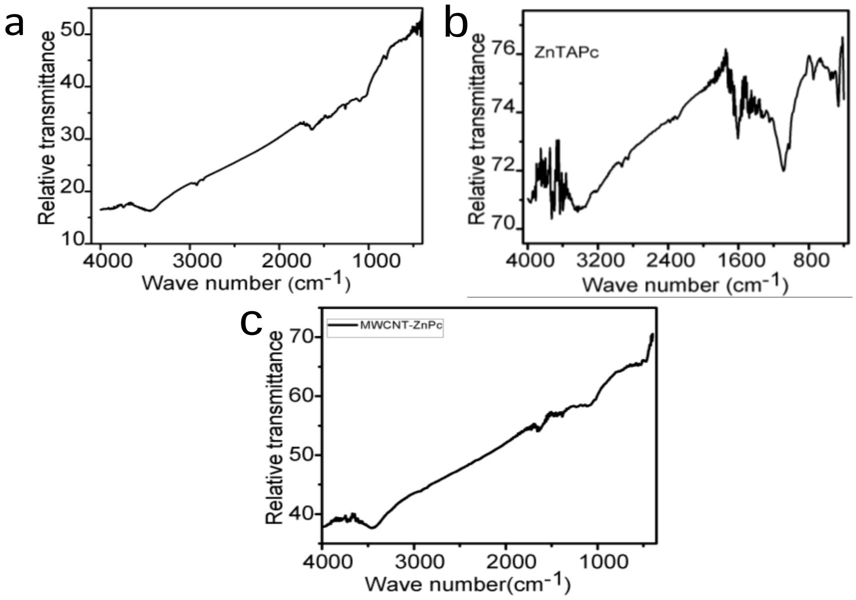

Figure 3. FT-IR spectra of (a) MWCNTs (b) Zn(II)TAPc and (c) Zn(II)TAPc-MWCNT

3.3. Powder X-Ray Diffraction studies

Figure 4 displays the XRD patterns of oxidized MWCNTs, Zn(II)TAPc and Zn(II)TAPc–MWCNTs. Powder X-ray Diffraction were examined at an angle of 2θ between 10–80 degrees. It was noted that there were no sharp peaks for MWCNTs revealing its amorphous nature. Due to the additional conjugation of the Zn(II)TAPc moiety, well-defined peaks at 08°, 10°, 18°, 25°, 36°, 39°, 43° and 48° were detected in Zn(II)TAPc indicating that the substance is crystalline. The Zn(II)TAPc–MWCNTs diffraction peaks (the curve c) were broad and weak in comparison to the curve b, in Figure 4, indicating a short crystal size or poor crystallinity of ZnTAPc in the ZnTAPc–MWCNTs hybrid materials. Additionally, the Zn(II)TAPc–

MWCNTs distinctive peaks weakened as a result the Zn(II)TAPc was evenly distributed across the surface of MWCNTs. All reflection peaks of Zn(II)TAPc–MWCNTs could be indexed as Zn(II)TAPc, indicating the Zn(II)TAPc nanostructures were successfully fabricated on the surface of MWCNTs.

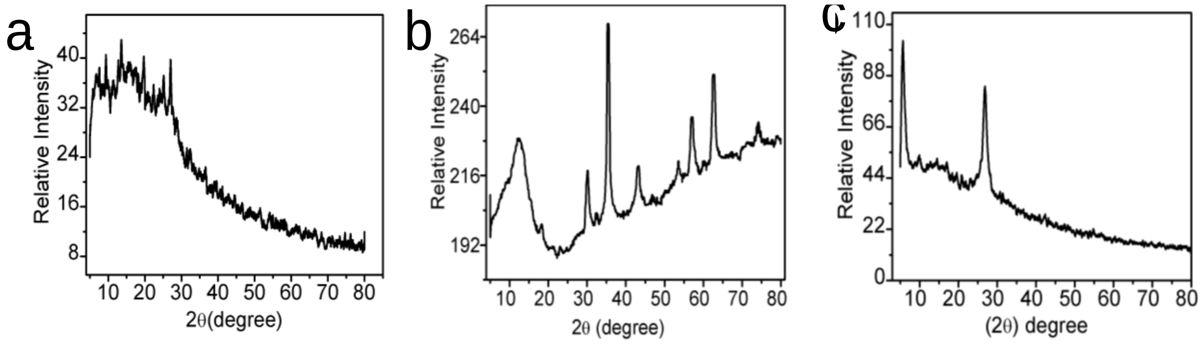

Figure 4. X-ray diffractograms of (a) MWCNTs, (b) Zn(II)TAPc, and (c) MWCNTs-Zn(II)TAPc

3.4. TGA analysis

TGA was used to calculate the covalent quantities of Zn(II)TAPc that were attached to the MWCNTs. Figure 5 shows the TGA measurements for pure MWCNTs, Zn(II)TAPc, Zn(II)TAPc–MWCNTs composite hybrid materials. Figure 5 depicts the percent mass loss as a function of temperature at a heating rate 10^0C min^{-1} in the presence of N_2 gas. At 800 ^{0}C, the hybrid Zn(II)TAPc and Zn(II)TAPc–MWCNT materials can be totally decompose with no inert residue left behind at 800^0C. There are clearly visible amounts of 38.4% of Zn(II)TAPc and 45.9% of Zn(II)TAPc–MWCNTs hybrid materials. In comparison, at this temperature 86.8% of MWCNTs pure. The amount of Zn(II)TAPc bonded to MWCNTs is estimated to be 55% by weight based on thermal degradation weights of Zn(II)TAPc–MWCNTs hybrid materials and pure MWCNTs at 800^0C [40].

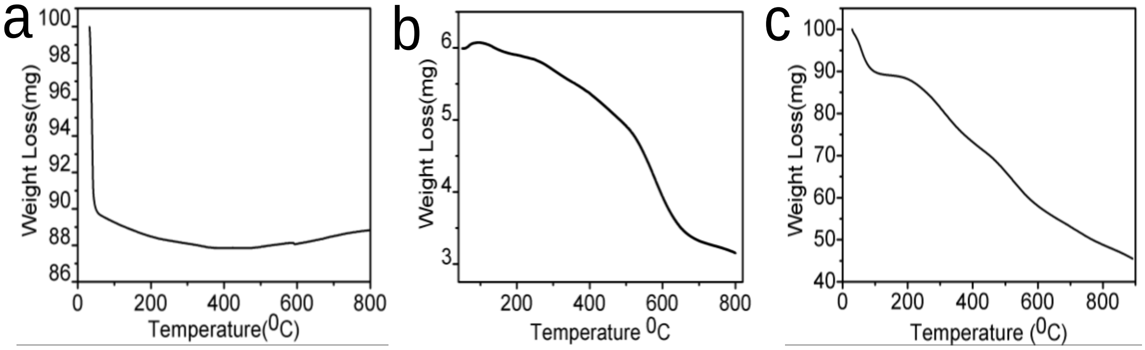

Figure 5. TGA curves of pure (a) MWCNTs, (b) Zn(II)TAPc, and (c) Zn(II)TAPc–MWCNTs hybrid materials

3.5. Surface morphology studies

SEM examination was used to study the surface morphology and structure of produced composite materials MWCNTs, Zn(II)TAc, and Zn(II)TAPc-MWCNTs (Figure 6). It is clear that the MWCNTs have rod-and-thread-like structure and the smooth, granular Zn(II)TAc surface of the MWCNTs embedded with Zn(II)TAPc has turned rough due to the ion exchange process. This demonstrated that MWCNTs successfully incorporated Zn(II)TAPc.

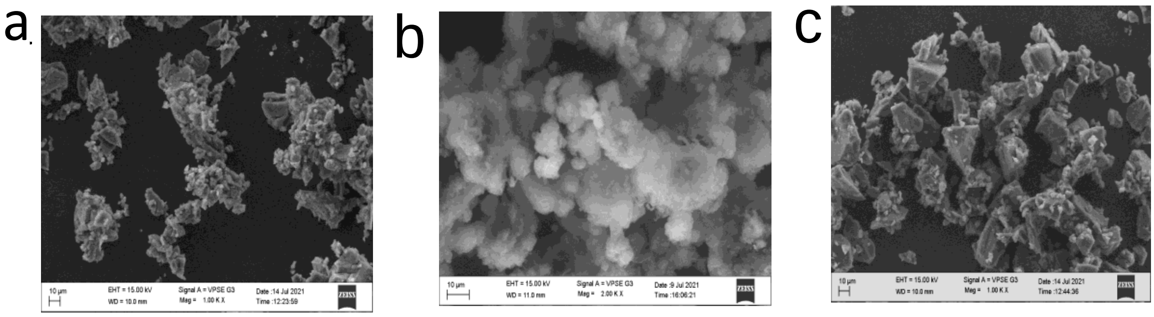

Figure 6. SEM images of (a) MWCNT and (b) Zn(II)TAPc (c) MWCNT-Zn(II)TAPc

3.5.1. Charge transfer behavior of modified electrode

The charge transfer behavior of bare electrode, Zn(II)TAPc/GCE and MWCNT-Zn(II)TAPc/GCE, are constructed electrode is done usually to observe variation occur in potential and current, among bare GCE, Zn(II)TAPc/GCE modified electrode and composite electrode. Here we studied this through $K_4[Fe(CN)_6]$ which acts as a redox probe. The modified GCE shows comparatively more I_{pa} and I_{pc} than bare GCE and Zn(II)TAPc/GCE this is due to MWCNT provides large surface area and composite electrode suggesting higher electron transfer between thin film and electrolyte system [41] is showed in Figure 7. The active surface area value for MWCNT-Zn(II)TAPc/GCE (0.00241×10^{-10} cm^2) is large as compared to Zn(II)TAPc/GCE (0.000913×10^{-10} cm^2) which was calculated by Randles-Sevick equation [42].

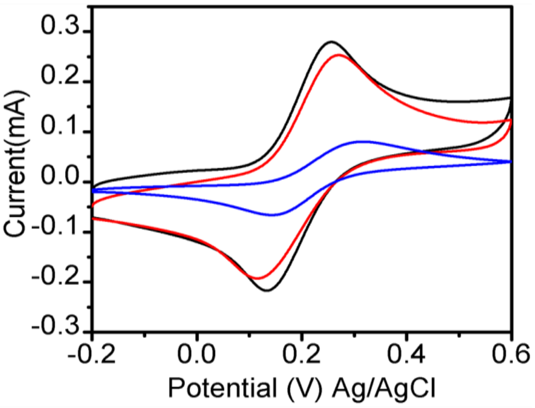

Figure 7. CVs of bare GCE (Blue Curve), Zn(II)TAPc/GCE (Red Curve), MWCNT-Zn(II)TAPc/GCE (Block Curve) in 1 mM $K_3[Fe(CN)_6]$ with scan rate of 50 mVs^{-1}

3.5.2. Electrochemical behavior on the modified electrodes

Figure 8 shows the electrochemical analysis of three different electrodes in PBS (pH=7.0) solution containing 0.1 µM of DA using an electrochemical work station with the potential range of -0.8 to 0.8V and a scan rate of 50 mVs^{-1}. The bare GCE which shows negligible current response, while the Zn(II)TAPc/GCE sensors have a significantly lower peak current response of 6.397 µA when compared to the MWCNT-Zn(II)TAPc/GCE sensors, which have a significantly higher current response of 8.90 µA. Furthermore, when varied concentration of DA are added to the phosphate buffer solution, the drop coated MWCNT-Zn(II)TAPc/GCE shows a increasing peak current response with a pronounced peak at 0.43 V. It suggests that the MWCNT-Zn(II)TAPc/GCE electron transfer rate is fast, which makes DA detection much easier [43].

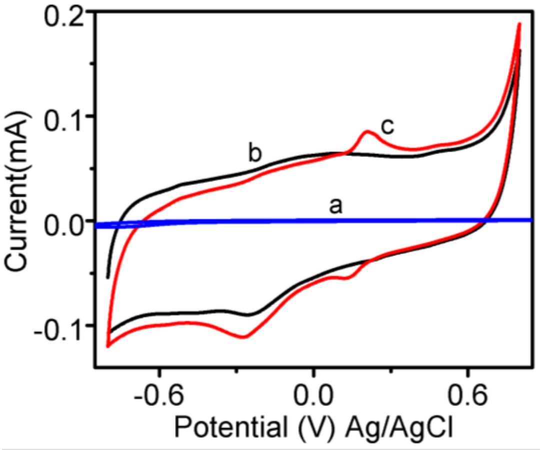

Figure 8. CV of (a) Bare GCE, (b) MWCNT-Zn(II)TAPc/GCE and (c) MWCNT-Zn(II)TAPc/GCE with 0.05 µM of DA in PBS pH 7.0, scan rate is 50 mVs^{-1}

3.5.3. Electrochemical determination of dopamine

Under aquatic conditions, DA was determined Electrochemically using modified MWCNT-Zn(II)TAPc/GC electrodes in PBS pH 7.0. The characteristic CVs of the modified MWCNT-Zn(II)TAPc/GCE in PBS pH 7.0 with and without DA at a scan rate of 50 mV s^{-1} in aquatic environment are shown in Figure 9. In the measured potential range -0.4 to 0.8 V in PBS. The unmodified GCE did not show any characteristic peak, the modified MWCNT-Zn(II)TAPc/GCE exhibits a well-defined and reversible pair of redox peaks at 0.43 V with the addition of various amount of DA. In this experiment, the DA oxidation peak current increased considerably at the MWCNT-Zn(II)TAPc/GCE, and the oxidation peak potential shifted to the negative potential side from 430 mV to 390 mV. This reveals that MWCNT-Zn(II)TAPc has a peak around 430 mV, which is due to the huge surface area of MWCNT. This raises peak current and decreases over potential, and as a result, act as a better electro-active catalyst for DA oxidation than without modified GCE. The analytical profile of the composite modified electrode was shows long linear range, good sensitivity and LOD, the linear range is 0.1 µM to 1.2 µML^{-1} with LOD is 0.0333 µML^{-1}, sensitivity of 14.063 µAµM respectively [28].

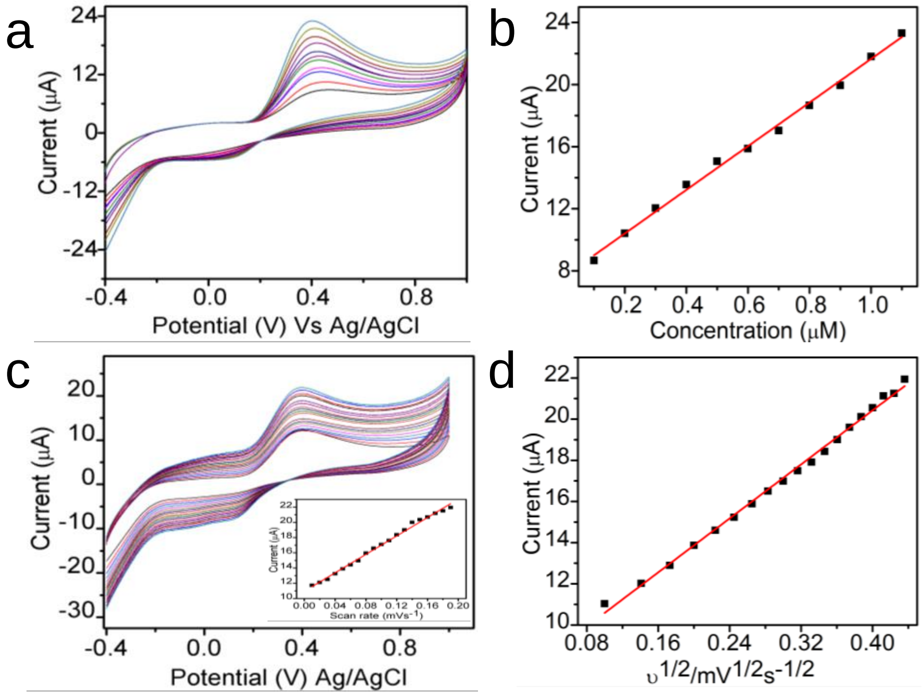

Figure 9. A) CVs of MWCNT-Zn(II)TAPc/GCE (a) different concentration of dopamine (0.1 µM to 1.2 µM) in PBS (pH 7), (b) linear plot of concentration Vs peak current, (c) at different scan rates (from 10 to 200 mVs^{-1}). Inset: plot of scan rate vs. peak current, (d) square root of scan rate vs. peak current

3.5.4. Effect of Scan rate

By observing the CV at various scan rate of 10-200 mVs^{-1}, the mass transfer behavior of the DA at the modified MWCNT-Zn(II)TAPc/GC electrodes was assessed. The CVs for the 1.0 µML^{-1} of DA on MWCNT-Zn(II)TAPc/GC electrodes in PBS (pH 7.0) are shown in Figure 9c for various scan rates. The electrochemical results at MWCNT-Zn(II)TAPc/GC electrodes demonstrated an increasing both anodic (I_{pa}) and cathodic (I_{pc}) peak current response, linear increase with a small shift in the anodic as well as cathodic peak potential slightly towards positive and negative potentials respectively. Figure 9d shows the straight-line relationship for the plot of peak current against square root of scan rate which suggests that the oxidation of DA electrolyte on the drop coated GCE follow diffusion-controlled mass transfer phenomena. The linear equation for the plot of peak current vs scan rate and peak current vs. square root of the scan rate at MWCNT-Zn(II)TAPc/GCE. A linear relationship was observed with the square root of the scan rate vs. peak current $i_{pa} = 3.328\, v^{1/2} + 7.054$, $R^2 = 0.9995$.

3.5.5. Electrochemical sensing of uric acid

The composite sensor as expected, the blank solution (pH 7) in the in Figure 10a does not contain any redox peaks. A well-defined and redox peak located at 418 mV vs. SCE with the addition of various amount of UA, ranging from 0.05 µM to 1.2 µML^{-1}, with a linear relationship between the peak currents and the different concentrations. For MWCNT-Zn(II)TAPc/GCE a well-established oxidation peaks was also detected, indicating that the bioanalyte (UA) oxidation reaction occurred at surface of the electrode. These occurrences provided unmistakable proof of the MWCNT-Zn(II)TAPc/GCE catalytic impact on the oxidation of uric acid [22,25]. The MWCNT-Zn(II)TAPc/GCE linear response to varying UA concentrations vs cathodic peak current (I_{pc}); Y= 0.515(UA)+0.593 with correlation coefficient of R^2=0.998 (Figure 10b). The LOD and LOQ were calculated by the equations LOD = 3S/M and LOQ = 10S/M where ‘S’ is the standard deviation and ‘M’ is the slope obtained from the calibration plots and found to be 0.0166 µM [30,44].

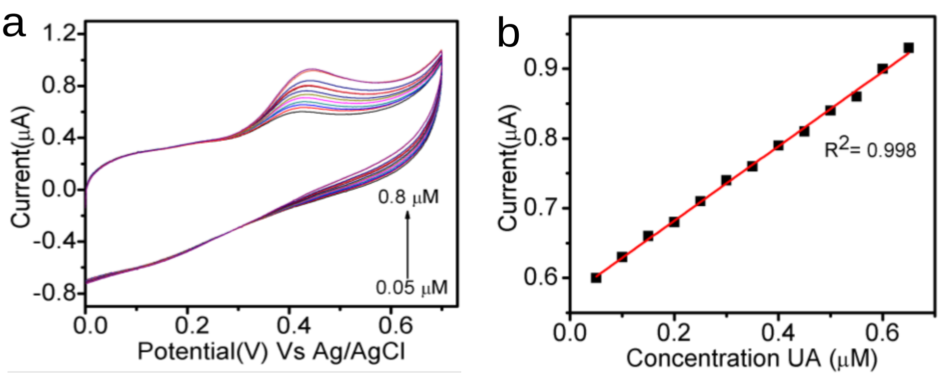

Figure 10. Cyclic voltammogram of MWCNT-Zn(II)TAPc modified GCE at (a) different concentrations of UA 0.05 µM to 1.2 µM and (b) inset linear graph of current vs. concentrations

3.5.6. Effect of Scan rate

Cyclic voltammetry was used to investigate the effect of scan rate on the electrochemical behavior of a composite GCE with analyte in PBS (pH 7.0) (Figure 11).

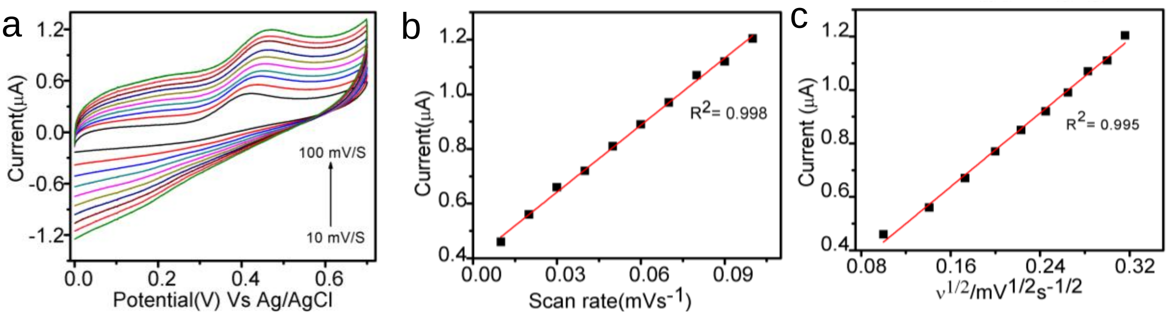

Figure 11. CV on MWCNT-Zn(II)TAPc in PBS (pH=7) electrolyte, (a) With different scan rates, (b) Linear plot of I_{pc} vs. scan rate, (c) Inset plot of I_{pc}/square root of scan rate

The anodic peak currents of MWCNT-Zn(II)TAPc/GCE are linearly proportional to the scan rates ranging from 10 and 100 mVs^{-1}, demonstrating that the electroanalyte reaction processes are surface controlled process rather than a diffusion-controlled [3,4,44]. The regression equations for the oxidation of UA can be expressed as follows: I_{pa} (µA) = 3.446 + 0.0867 V (mVs^{-1}) (R^2 = 0.995).

3.5.7. Electrocatalytic oxidation of AA using MWCNT-Zn(II)TAPc/GCE modified electrode

The electrocatalytic activity of MWCNT-Zn(II)TAPc electrode towards AA was investigated, and the results are shown in Figure 12. In the absence of AA (inset Figure 12a), no oxidation and reduction peak current change was observed. After adding different concentrations of AA from 0.1 to 1.5 μML^{-1}, the oxidation peak current increases proportional with increasing AA concentration, while the reduction peak current decreases. It was shown that the oxidation of AA can be catalyzed by composite sensors, and that the composite sensors have good electrocatalytic activity towards AA oxidation. The composite modified electrode also exhibits good results, sensitivity 0.515 $\mu A \mu M^{-1,}$ LOD is 0.033 $\mu molL^{-1}$ and R^2 = 0.997 [45].

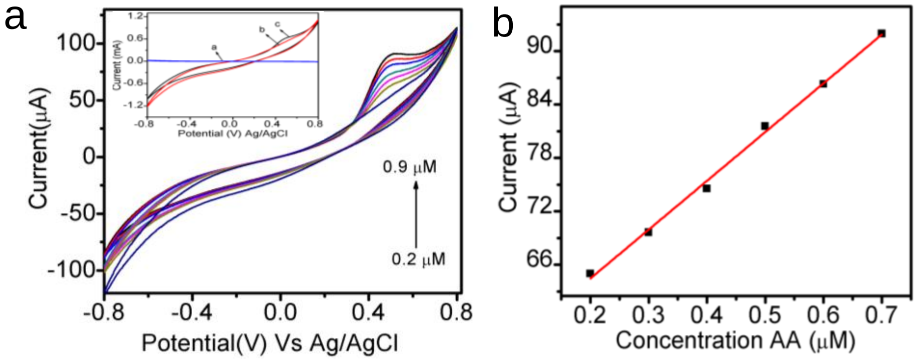

Figure 12. CVs of MWCNT-Zn(II)TAPc in PBS pH 7.0 (a) different concentration of AA 0.2 to 0.9µM at a scan rate of 50 mV/s and (b) Inset linear graph of current Vs concentration AA (µM)

3.5.8. Effect of Scan rate

The CVs on the MWCNT-Zn(II)TAPc GCE in the PBS (pH 7.0) were measured at different scan rates (10-200 mVs^{-1}). The electrochemical investigation demonstrates that the peak current shifts to the positive side, the peak potential shifts slightly negative, and the peak current increases while scan rate increases. In the 10 to 200 mV/s region, a linear relationship was observed between the peak current and the square root of the scan rate. The linear plot of peak current vs scan rate followed the straight-line equation represented by: I_{pa}= $190.208v^{½}$+35.538, with correlation of coefficient R^2=0.991 (Figure 13b). The linear relationship between peak current and scan rate shows that the modified sensor is undergoing diffusion-controlled mass transfer process.

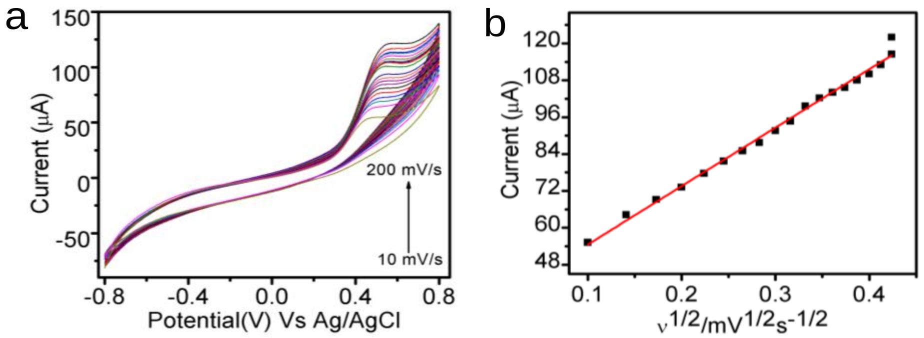

Figure 13. CVs of MWCNT-Zn(II)TAPc/GCE modified electrode in pH 7.0 PB solution at Different scan rates: (A) 10 to 200 mVs^{-1}. Inset: the relation between the anodic peak Currents and square root of scan rates

3.5.9. Analytes oxidation reactions

Oxidation-reduction reactions of dopamine, uric acid oxidation, and ascorbic acid is shown in Scheme 1. Table 1 shows the practical values for the determination of DA, AA and UA on MWCNT-Zn(II)TAPc modified GCE in PBS (pH 7.0).

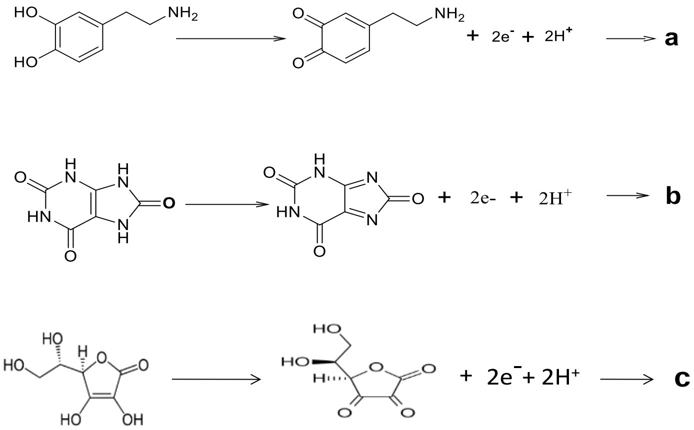

Scheme 1. Analytes oxidation-reduction reactions a) Dopamine oxidation, b) Uric acid oxidation, c) Ascorbic acid oxidation

Table 1. Practical values of determination of DA, AA and UA on MWCNT-Zn(II)TAPc/GCE in PBS (pH 7.0)

Sensitivity (μAμM^{-1} cm^{-2})			**LOD (μmolL^{-1})**			**Linear range(μmolL^{-1})**			**Ref.**
DA	AA	UA	DA	AA	UA	DA	AA	UA	
0.96	0.89	3.11	1.4	7.6	0.6	2-70	10-250	2.0-50	[46]
0.006	0.10	0.03	0.17	0.11	-	0.05-470	0.5-1300	0.2-100	[47]
0.33	0.18	0.038	0.25	0.3	2.0	1-10	5-105	0-110	[48]
0.179	-	0.517	1.33	-	1.0	4-32	-	2-14	[27]
0.27	56.03	53.06	0.0166	0.006	0.006	0.05-0.8	0.05-10	0.02-50	This work

3.5.10. Interference study

The selectivity of MWCNT-Zn(II)TAPc/GCE was determined by measuring 50 µmol L^{-1} DA, 100 µmolL^{-1} AA and 50 µmolL^{-1} UA in PBS pH 7.0, each containing significant biological compounds was set at roughly +5% relative error. Table 2, K$^+$, Na$^+$, Mg$^+$, Ca$^+$, glucose and sucrose showed little substantial influence [49]. However, Cu^{2+} and Fe^{2+}, on the other hand, had only a minor effect on the detection of DA, AA and UA. Furthermore, epinephrine had a significant influence on their determination, which can be attributed to their identical peak potentials to DA, AA and UA. As a result, the developed sensor had great selectivity for their detection of biomolecules coexisting with the majority of interference compounds.

Table 2. Interference study results

Interferent	**Concentration/µmolL^{-1}**	**Signal change**		
		DA%	**AA%**	**UA%**
K$^+$	6000	1.30	0.04	-1.14
Na$^+$	6000	0.09	-0.06	0.07
Mg^{2+}	3000	1.43	-1.32	-1.18
Ca^{2+}	3000	-1.34	1.05	0.60
Cu^{2+}	1000	2.72	5.74	1.34
Fe^{2+}	1000	5.60	-1.42	0.23
Glucose	1000	-0.08	-0.18	1.08
Sucrose	100	-1.06	1.15	-0.06
Epinephrine	50	10.35	4.25	1.08

3.5.11. Real and synthetic sample analysis

After being diluted by 10 times with 0.1 M PBS (pH 7), human urine samples were immediately examined.

Table 3. Determination of DA, AA, and UA levels in urine samples using the MWCNT Zn(II)TAPc/GCE in PBS (pH 7) (Each result was average of three determinations)

Samples	**Analyte**	**Spiked DA/µM**	**Found DA/µM**	**RSD%**	**Recovery %**
Sample 1	DA	10	9.9	99.0	1.3
	AA	50	50.3	100.6	1.5
	UA	20	19.7	98.5	2.2
Sample 2	DA	10	10.1	101.0	1.4
	AA	50	49.8	99.6	3.1
	UA	20	19.8	99.5	2.4
Sample 3	DA	10	10.2	102.0	2.2
	AA	50	49.2	98.4	2.3
	UA	20	20.3	101.5	3.2

The conventional addition approach was used to determine the composition of the bioanalyts. The diluted samples indicated above were spiked with varying concentrations of DA, AA, and UA and then detected to ensure accuracy of the results. The recovery of the spiked samples ranged from 98.0% and 102.0% (Table 3), demonstrating the successful use of the prepared electrochemical sensors to determination of DA, AA, and UA in the real biological samples

4. CONCLUSION

In conclusion, the composite phthalocyanine structure was studied using a various physico-chemical techniques. The resulting compounds display increased thermal stability and solubility in DMF and DMSO as well as maximal UV light absorption from 200 to 700 nm. In this article, MWCNT-Zn(II)TAPc was made to conduct individual electrochemical analysis of DA, AA and UA using environmentally friendly electrochemical technique. Due to its exceptional electro-catalytic characteristics and distinctive structural features, the biocatalyst can be oxidized with high electrocatalytic activity. MWCNT-Zn(II)TAPc/GCE modified sensors shows greatly catalyzes the oxidation of bioanalytes that showed high response, could be used for the individual sensing of biomolecules with high sensitivity and electrochemical stable. Moreover, the sensor based on it shows good electrocatalytic activities to DA, UA and AA with wider linear detection range, lower detection limit, good sensitivity of biomolecules 0.033 µM, 0.066 µM, 0.016 limit of quantification were 0.09 µM, 0.198 µM, 0.048 µM. The composite modified electrode shows outstanding anti-interference ability, stability and reproducibility.

Acknowledgments

The author Dr. Malathesh Pari are thankful to Sahyadri Science College Shivamogga for providing electrochemical work stations and spectral facilities.

Declarations of interest

The authors declare no conflict of interest in this reported work.

REFERENCES

[1] K.R.V. Reddy, J. Keshavayy, B.E.K. Swamy, M.N.K. Harish, H.R. Mallikarjun, and B.S. Sherigar, Dyes and Pigments 80 (2009) 1.

[2] B.S. Jilani, C.D. Mruthyunjachari, M. Pari, and K.R.V. Reddy, Sens. Actuators B 301 (2019) 127078.

[3] J. Griffiths, J. Schofield, M. Wainwright, and S.B. Brown, Dyes and Pigments 33 (1997) 65.

[4] K.M. Pradeep, K.R.V. Reddy, M.N.K. Harish, B. Chidanada, B.J. Madhu, C.D. Mruthyunjayachari, and S.D. Ganesh, Synthetic Metals 79 (2013) 185.

[5] M. Pari Mounesh, B.S. Jilani, and K.R.V. Reddy. Anal. Bioanal. Electrochem. 11 (2019) 460.

[6] K.R.V. Reddy, M.N.K. Harish, Fassiulla, M.H. Moinuddin Khan, and J. Keshavayya J. Fluor. Chem. 128 (2007) 1019.

[7] K.M. Pradeep, K. Musturappa, V.K.R. Reddy, M.N.H. Kotresh, B.C. Basappa, D. Ganesh, M.B. Jayanna, and M.C. Devendrachari, J. Inorg. Organomet. Polym. 23 (2013) 958.

[8] S.L. Jain, J.K. Joseph, S. Singhal, and B. Sain, J. Mol. Catal. A 268 (2007) 134.

[9] Y. Ipek, H. Dincer, and A. Koca, Sens. Actuators B 193 (2014) 830.

[10] D.A. Geraldo, C.A. Togo, J. Limson, and T. Nyokong, Electrochim. Acta 53 (2008) 8051.

[11] S. Centane, O.J. Achadu, and T. Nyokong, Electroanalysis 29 (2017) 1.

[12] A. Alonso, B. Etxaniz, and M.D. Martinez, Food Additives and Contaminants 9 (1992) 111.

[13] B.C. Marshall, and W.C. Koch, Paediatric Drugs 11 (2009) 309.

[14] M. Sharland, S. Luck, P. Griffiths, and M. Cotton. Adv. Exp. Med. Biol. 697 (2011) 243.

[15] A.K. Field, M.E. Davies, C. Dewitt, H.C. Perry, R. Liou, J. Germerhausen, J.D. Karkas, W.T. Ashton, D.B.R. Johnson, and R.L. Toiman, Proc. Natl. Acad. Sci. USA 80 (1983) 4139.

[16] D. Faulds, and R.C. Heel, Ganciclovir. J. Drugs 39 (1990) 597.

[17] D. Sun, Y. Zhang, F.R. Wang, K.B. Wu, J.W. Chen, and Y.K. Zhou, Sens. Actuators B 141 (2009) 641.

[18] H.R. Zare, N. Nasirizadeh, and M.M. Ardakani, J. Electroanal. Chem. 577 (2005) 25.

[19] A.S. Soper, L.B. Mc Gown, and I.M. Warner, Anal. Chem. 66 (1994) 428.

[20] A. Roychoudhury, K.A. Francis, J. Patel, S.K. Jha, and S. Basu, RSC Adv. 10 (2020) 25487.

[21] R. Zhang, G.D. Jin, D. Chen, and X.Y. Hu. Sens. Actuators B 138 (2009) 174.

[22] Y.F. Zhao, Y.Q. Gao, D.P. Zhan, H. Liu, Q. Zhao, Y. Kou, Y.H. Shao, M.X. Li, Q.K. Zhuang, and Z.W. Zhu, Talanta 66 (2005) 51.

[23] B.J. Venton, and R.M. Wightman, J. Anal. Chem 75 (2003) 414A.

[24] K.H. Xue, F.F. Tao, S.Y. Yin, W. Shen, and W. Xu. Chem. Phys. Lett. 391 (2004) 243.

[25] L.R. Junior, J.C.B. Fernandes, and G.O. Neto. J. Electroanal. Chem. 481 (2000) 34.

[26] X.H. Lin, Q. Zhuang, J.H. Chen, S.B. Zhang, Y.J. Zheng. Sens. Actuators B 125 (2007) 240.

[27] L.M. Niu, K.Q. Lian, H.M. Shi, Y.B. Wu, W.J. Kang, S.Y. Bi, Sens. Actuators B 178 (2013) 10.

[28] M. Pari, K.R.V. Reddy, and K.B.F. Chandrakala, Sens. Actuators A 316 (2020) 112377.

[29] L. Afroz, M.H.M. Khan, H.M. Vagdevi, M. Pari, J. Emergent Mater. 5 (2022) 1133.

[30] N. Ranjitha, G. Krishnamurthy, H.S.B. Naik, M. Pari, L. Afroz, K.R. Sumadevi, and M.N. Manjunatha, Inorganica Chim. Acta 543 (2022) 121191.

[31] M. Pari, K.R.V. Reddy, Anal. Bional. Electrochem. 11 (2019) 1383.

[32] W.J. Kang, L.M. Niu, N. Ma, Chinese Chem. Lett. 20 (2009) 221.

[33] S. Rajappa, P.G. Shivarathri, M.L.A. Kumari, D.K. Swamygowda, and M.C.D. Chari, Surfaces and Interfaces 29 (2022) 101720.

[34] Fasiulla, and M.P. Yashoda, Orient. J. Chem. 33 (2017) 2530.

[35] M.H.M. Khana, K.R.V. Reddy, J. Keshavayya, Fasiulla, and S. Raghavendra, Green Chem. Lett. Rev. 2 (2009) 77.

[36] B.N. Achar, K.S. Lokesh. J. Organometallic Chem. 689 (2004) 3357.

[37] S.M. Sudhakara, M.C. Devendrachari, H.M.N. Kotresh, and F. Khan, J. Electroanal. Chem. 884 (2021) 115071.

[38] I. Mohammed, M. Nemakal, V.A. Sajjan, D.B. Puttappashetty, and L.K. Sannegowd, J. Electroanal. Chem. 826 (2018) 96.

[39] V.A. Sajjan, S. Aralekallu, M. Nemakal, M. Palanna, C.P.K. Prabhu, L.K. Sannegowda, Inorganica Chim. Acta 506 (2020) 119564.

[40] K.G.K. Shambhulinga, N. Manjunatha, M. Imadadulla, and K.S. Lokesh, Surf. Interfaces 15 (2019) 19.

[41] C. Raril, and J.G. Manjunatha, J. Anal. Sci. Technol. 11 (2020).

[42] V.N. Krishnanaik, G. Krishnamurthy, M. Pari, I. Venugopala, N. Ranjitha, and N. Naik Biointerface Res. Applied Chem. 13 (2023) 531.

[43] S.K. Gopinath, M. Pari, A.M. Rudrannagari, I.B. Kattebasaveshwara, and S.K. Halappa, Biointerface Res. Applied Chem. 11 (2021) 11390.

[44] M. Pari, B.S. Jilani, and K.R.V. Reddy, Anal. Bioanal. Electrochem. 11 (2019) 460.

[45] C. Wang, R. Yuan, Y. Chai, S. Chen, F. Hu, and M. Zhang, Anal. Chim. Acta 741 (2012) 15.

[46] A.A. Ensafi, M. Taei, T. Khayamian, and A. Arabzadeh. Sens. Actuators B 147 (2010) 213.

[47] L. Lin, J. Chen, H. Yao, Y. Chen, Y. Zheng, and X. Lin, Bioelectrochemistry 73 (2008) 11.

[48] B.S. Jilani, M. Pari, and K.R.V. Reddy, Anal. Bioanal. Electrochem. 11 (2019) 892.

[49] Y. Li, and X. Lin, Sens. Actuators B 115 (2006) 134.